Anterior Cervical Corpectomy Non-Fusion Model Produced by a Novel Implant

Authors' Contribution:
Study Design A
Data Collection B
Statistical Analysis C
Data Interpretation D
Manuscript Preparation E
Literature Search F
Funds Collection G

ABEF 1 **Jun Dong**
BCG 1 **Meng Lu**
D 2 **Baobao Liang**
D 3 **Xu Zhai**
F 1 **Jie Qin**
AEG 1 **Xijing He**

1 Department of Orthopaedics, Second Affiliated Hospital of Xi'an Jiaotong University, Xi'an, Shaanxi, P.R. China
2 Department of Plastic Surgery, Second Affiliated Hospital of Xi'an Jiaotong University, Xi'an, Shaanxi, P.R. China
3 Department of Emergency, Second Affiliated Hospital of Xi'an Jiaotong University, Xi'an, Shaanxi, P.R. China

Corresponding Author: Xijing He, e-mail: xijingh@sina.cn
Source of support: Ph.D. Programs Foundation of Ministry of Education of China (No.: 20120201130009) and Innovation Project Foundation of Science and Technology of Shaanxi Province (No.: 2011KTCL03-17) were received in support of this work. No benefits in any form have been or will be received from a commercial party related directly or indirectly to the subject of this manuscript

Background: Anterior cervical corpectomy and fusion are frequently used in the treatment of cervical spinal disease. However, the range of motion (ROM) of the operative level is unavoidably lost due to fusion. This study aims to establish an anterior cervical corpectomy goat non-fusion model and to evaluate the ROM of adjacent and operative levels.

Material/Methods: Six adult-male goats (*in vivo* group) and twelve adult-male goat cervical spine specimens (randomly divided equally into intact group or *in vitro* group) were included. The non-fusion model was established by implanting a novel implant at C_4 level. Imagiological examinations for the *in vivo* group were performed to inspect the position of the implant and spinal cord status. Specimens were harvested six months after the operation. Biomechanical testing was conducted to obtain the ROM in flexion-extension, lateral bending, and axial rotation at upper adjacent level (C_{2-3}), operative levels (C_{3-4} and C_{4-5}) and at C_{2-5}. Specimens in the intact group were first tested as intact and then tested as fixed and became the fixation group.

Results: Imagiological examinations revealed that the position of the implant and the spinal cord status were good. The specimens in the *in vivo* and *in vitro* groups had significantly decreased C_{2-3} ROM, increased C_{3-4} and C_{4-5} ROM and similar C_{2-5} ROM compared with the fixation group.

Conclusions: This study presents a novel method for potential non-fusion treatment strategies for cervical spinal disease. However, improvement of this model and additional studies are needed.

MeSH Keywords: **Biomechanical Phenomena • Cervical Vertebrae • Prostheses and Implants**

Full-text PDF: http://www.medscimonit.com/abstract/index/idArt/897244

📄 2944   ⊞ —   📊 12   📑 21

Background

Anterior cervical corpectomy and fusion (ACCF) is frequently used in the treatment of cervical spinal disease [1,2]. Although this procedure has been reported to have positive outcomes, operative level motor function is inevitably lost when three or more cervical vertebras are fused during the procedure [3]. Patients who undergo ACCF often complain of neck pain or numbness of upper limbs even after long-term follow-up [4]. Some patients experience degeneration of the adjacent upper or lower segments, a condition known as adjacent segment disease (ASD) [5]. Possible reasons for ASD may be ROM redistribute into the adjacent spinal segment that increases pressure inside the adjacent discs and facet joints, further accelerating degeneration [6].

As non-fusion technology develops, motion preservation devices, such as the artificial cervical disc, have demonstrated their ability to prevent ASD [7,8]. However, artificial cervical disc is limited by its inability to reconstruct the height of vertebra, and hence cannot be used when cervical corpectomy must be performed in the treatment of diseases, such as ossification of posterior longitudinal ligament (OPLL) [9]. Currently, the investigation of intervention strategies for ASD after ACCF is lacking and further *in vivo* assessments are limited by the absence of an ideal cervical corpectomy non-fusion animal model. To date, there has been a paucity of motion preservation devices used for the investigation of this problem. An ideal model would restore the motion of the intervertebral space not only *in vitro* but also *in vivo*. To address this issue, we have designed a non-fusion implant model in goats. Our study used an *in vitro* and *in vivo* cervical corpectomy non-fusion goat model and tested the model's range of motion (ROM) for operative levels (C_{3-4} and C_{4-5}) and the upper adjacent level (C_2).

Material and Methods

A Non-fusion implant

The implant, produced by three-dimensional (3D) metal printing technology (Bright Laser Rapid Prototyping Technology Co. Ltd., Xi'an, China), was made of Ti6Al4V alloy. It consisted of two artificial discs, one artificial vertebra, and four self-tapping screws (Figure 1). The ROM between the disc and the vertebra was 10° in flexion, extension, and lateral bending, and 360° in axial rotation.

In vitro and *in vivo* cervical corpectomy non-fusion model

This animal experiment was performed following the principles of laboratory animal care of National Research Council Guide, as well as the protocols approval by the ethical committee of Xi'an Jiaotong University. Twelve adult-male goat cervical spine specimens (C_1–C_7) and six adult-male goats (38.5±2.1 kg) were included in this study (provided by animal surgery center, Second Affiliated Hospital of Xi'an Jiaotong University).

The 12 cervical spine specimens were randomly divided into an intact group and an *in vitro* group with six specimens in each group. Muscle and peripheral soft tissue were removed with caution, keeping the ligament and capsule of the facet joint intact. Specimens of the *in vitro* group had a cervical corpectomy performed at C_4 level. A 15 mm width incision for decompression was made by a bone rongeur. The C_{3-4} and C_{4-5} discs were removed by a pituitary rongeur. The implant was assembled and then implanted at the C_4 level followed by screw fixation at C_3 and C_5, respectively. The specimens were preserved under minus 20°C condition before biomechanical testing.

The operation for the *in vivo* group was performed under aseptic conditions. The six male-adult goats had a 24-hours fast to empty their digestive tract. Before anesthesia, a venous channel was established via ear vein and a subcutaneous injection of atropine (0.02 mg/kg) was administered to reduce tracheal secretions. Equipment, such as negative pressure aspirator and sputum suction apparatus, were prepared for use as needed by nursing staff during the operation. Pentobarbital sodium (30 mg/kg) was injected via the venous channel for anesthesia. The process followed for the operation is presented in Figure 2.

X-rays (QDR-2000; Hologic, Waltham, MA.) were taken to confirm the implant was in a good position. Computed tomography (GE Medical Systems, Milwaukee, WI) with slice thickness of 0.625 mm was taken to observe the implant in detail by using 3D reconstruction modelling. Magnetic resonance imaging (MRI) of 1.5T (MAGNETOM Amira, Siemens, Germany) was taken to verify non-compression of the spinal cord. CT was also taken six months after the operation.

All the goats were raised in the animal care center of Second Affiliated Hospital of Xi'an Jiaotong University and were euthanized six months after the operation. The harvested cervical spine specimens (C_1–C_7) were kept under minus 20°C conditions prior to biomechanical testing.

Biomechanical testing

The specimens were thawed at room temperature before testing. C_1 and C_2 as well as C_6 and C_7 were fixed together by several nails for the enhancement of embedding. The ends of specimens were embedded vertically into two molds containing a mixture of N (3-dimethylaminopropyl)-1, 3-propylenediamine and bisphenol A-(epichlorhydrin) (1:1). Materials testing machine (MTS) (model MTS 858 Bionix, MTS Systems, Minneapolis, MN, USA) and an optoelectronic 3D motion capture
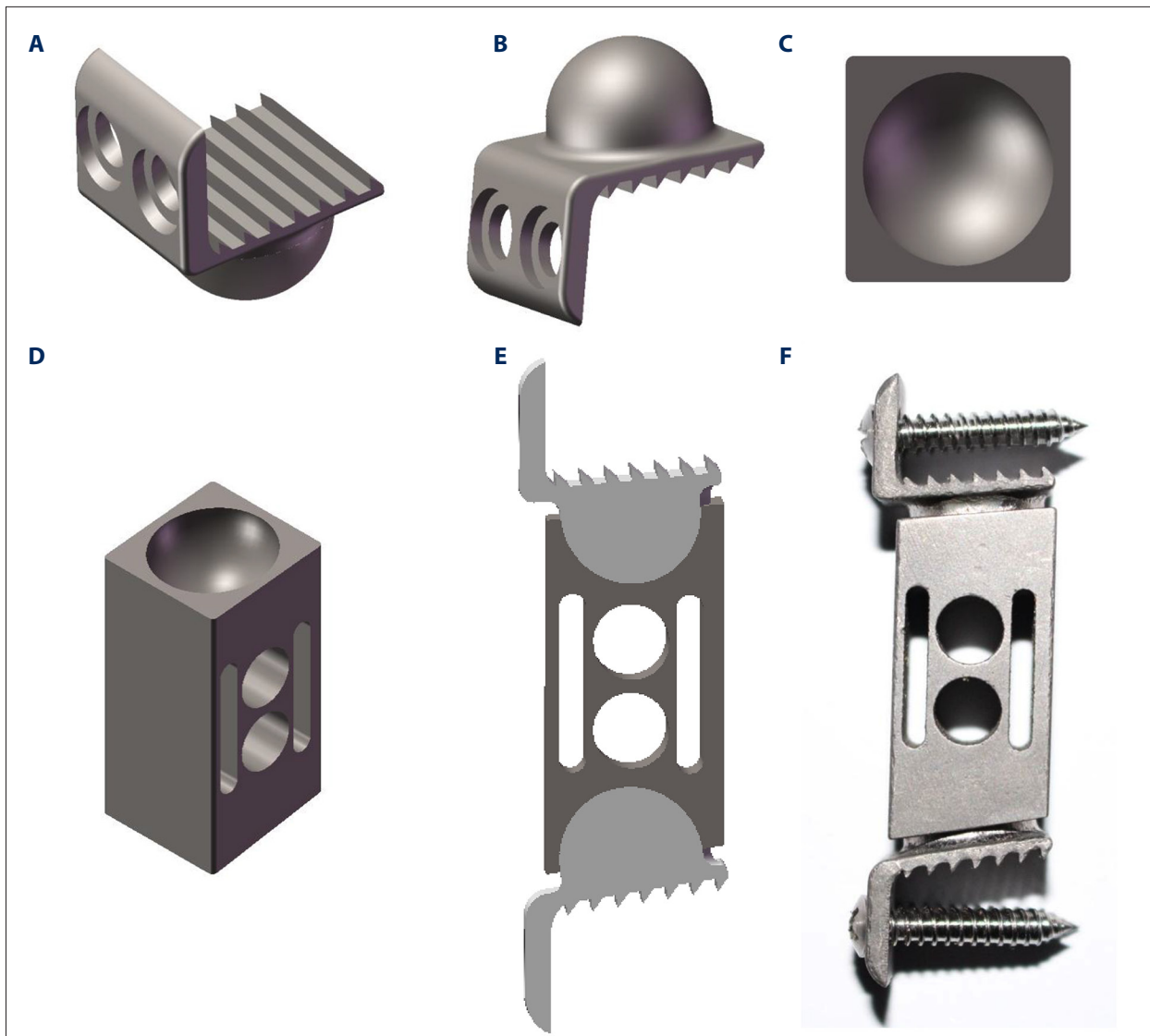
Figure 1. Photographs of the implant. (**A, B**) The disc with an anterior plate and an endplate. Two holes with a diameter of 3.5 mm placed inside the anterior plate for the screw fixation. The endplate with special structures, several dentate grooves on the surface, and a column with a height of 1 mm followed by a hemispheric articular head with a diameter of 12 mm. (**C, D**) The vertebra was a quadrangular column (33 mm-38 mm in length, 14 mm in width and 14 mm in depth), with a hemispheric articular fossa (12 mm in diameter) in the center of the two ends. (**E**) The angle between the anterior plate and the endplate was 84° in the upper disc and 100° in the lower disc. (**F**) To match the angle between the anterior plate and endplate, a 6° angle between the top surface and horizontal plane and a 10° angle between the bottom surface and horizontal plane were designed. Two long grooves and two holes laterally interpenetrate the artificial vertebra for the formation of a bony bridge. The self-tapping screws for fixation were 16 mm-18 mm in length, 3.0 mm-3.4 mm in diameter.

system with three cameras (Optotrack Certus, Northern Digital Inc., Waterloo, Canada) were used in the tests. The Optotrack Certus had a 3D precision of 0.1 mm, a measuring distinguishability of 0.01 mm and a sampling frequency of 100 Hz. The vertebras (C_2, C_3, C_4 and C_5) were attached with light-emitting diodes (LEDs) (Figure 3). The specimens had circulatory movement in flexion-extension, left-right bending, or left-right rotation axially when a 1.5 Nm was applied to its top by MTS. In total, five loading cycles were completed. The torque

and the angle were recorded by MTS. The instantaneous spatial locations of the LEDs were recorded by Optotrack Certus. The movement of LED was converted to ROM using MATLAB (MathWorks, Natick, MA, USA).

Specimens from the intact group, *in vitro* group, and *in vivo* group were tested. The specimens in the intact group were tested first as the intact group, then were fixed (from C_3 to C_5) by an anterior plate (Fule Science & Technology Development
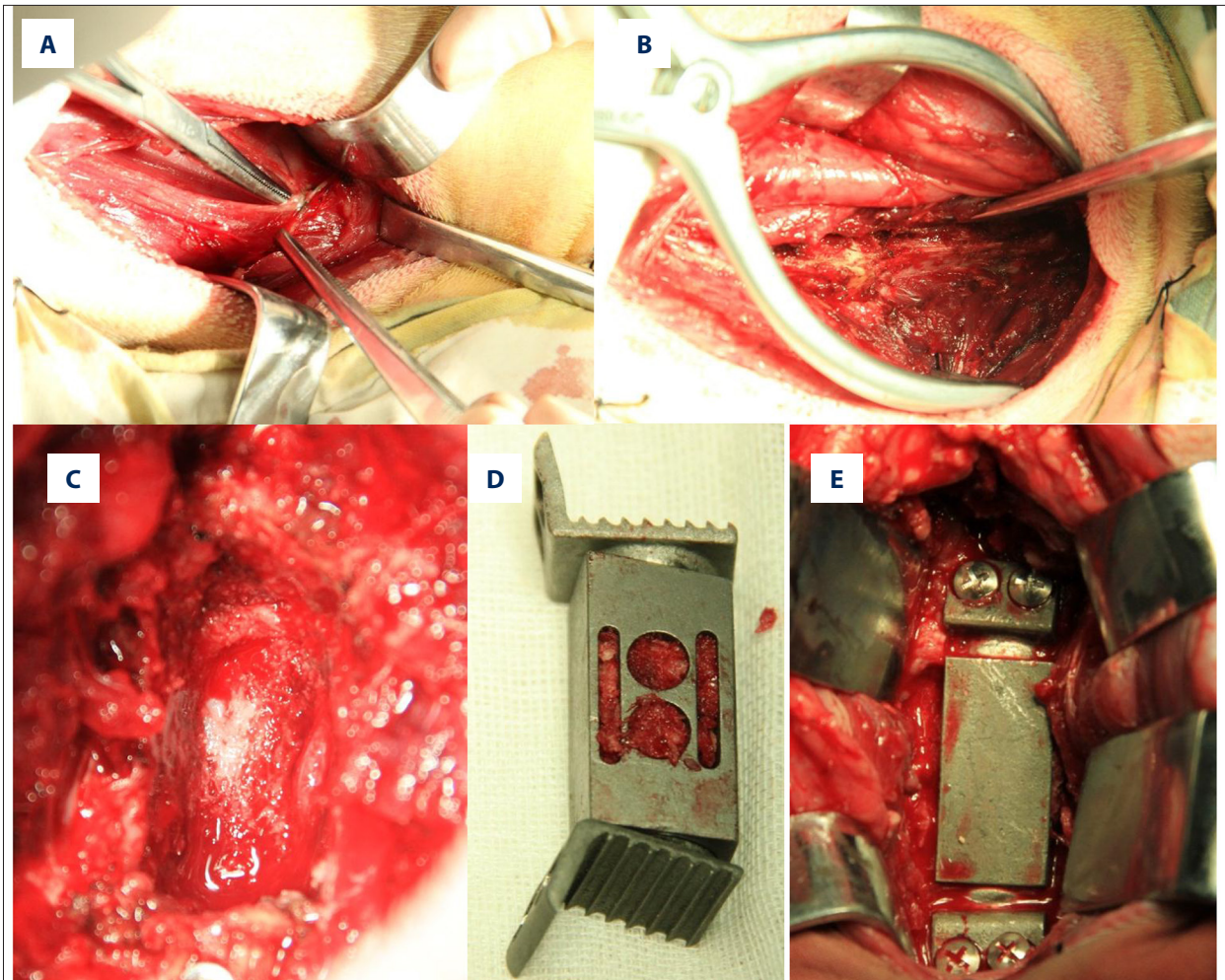
Figure 2. Process for establishing the *in vivo* model. Goats were placed supine after anesthetization. (**A**) Right-sided anterolateral approach was used. (**B**) Adequate exposure of C_3 to C_5 vertebra bodies was made. (**C**) Corpectomy at C_4 vertebra was performed. (**D**) Implant was filled with cancellous bone. The prosthesis was implanted at C_4 followed by screw fixation at C_3 and C_5 vertebra.
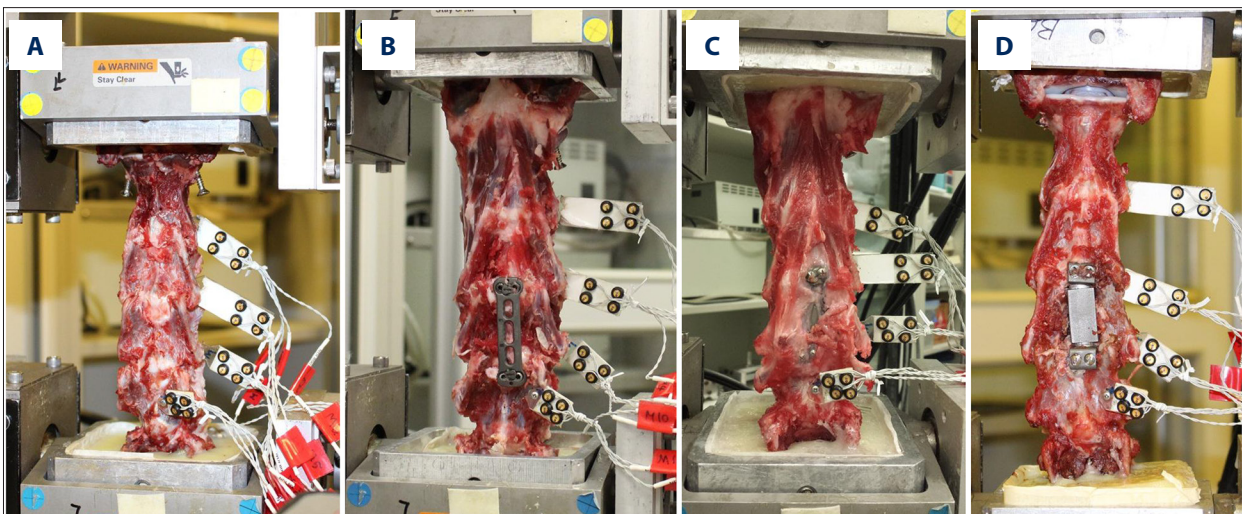

Figure 3. Photographs of biomechanical testing. (**A**) Intact group. (**B**) Fixation group. (**C**) *In vivo* group. (**D**) *in vitro* group.
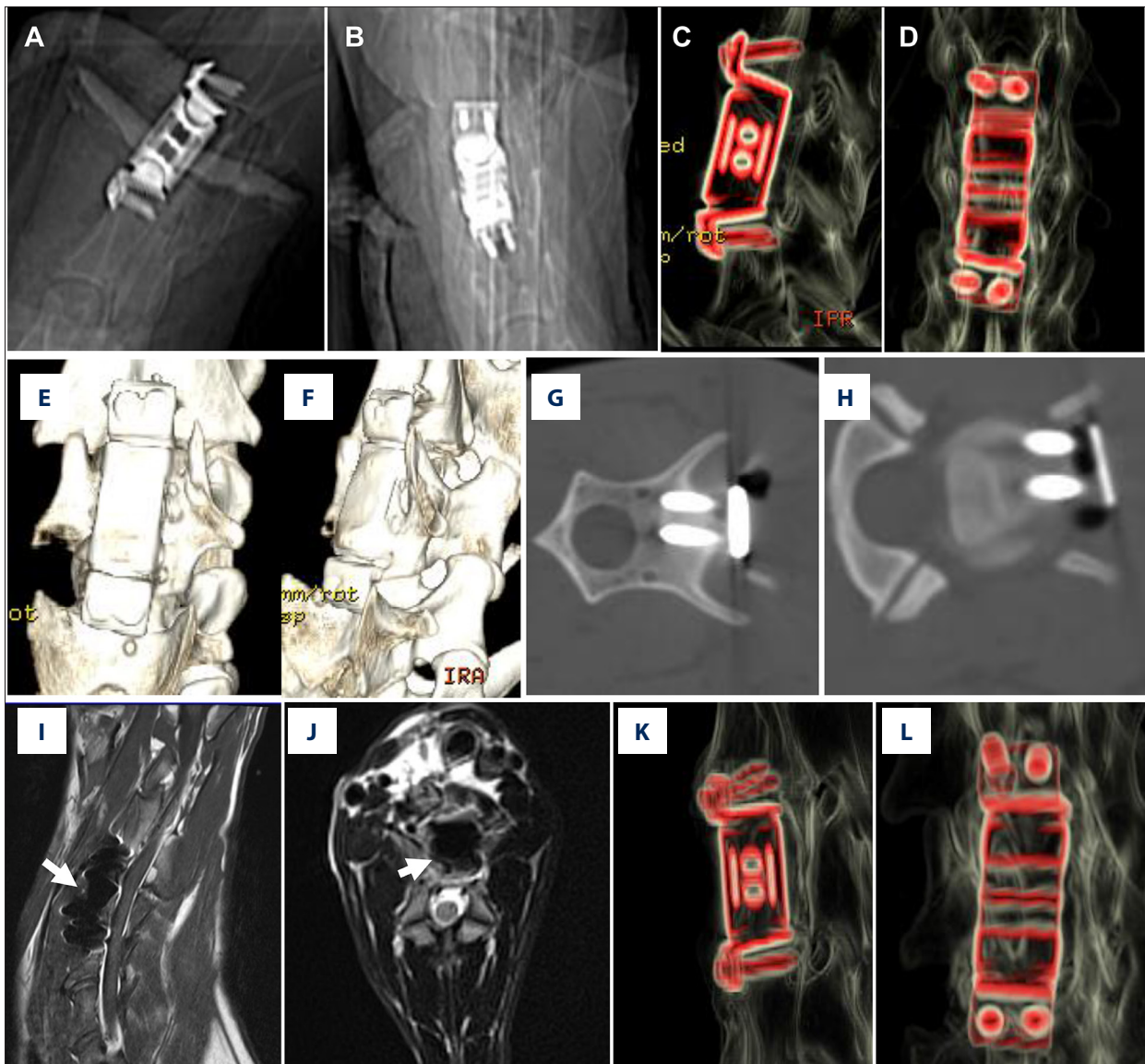
Figure 4. Images of the *in vivo* model. (**A**) Later view of postoperative X-ray. (**B**) Anteroposterior view of postoperative X-ray. (**C, D**) Hardware enhanced reconstruction of postoperative CT. (**E, F**) Reconstruction of postoperative CT. (**G**) Screws in C_3 vertebra body. (**H**) Screws in C_5 vertebra body. (**I**) Sagittal view of the postoperative T_2 image, the implant (white arrow) did not compress the spinal cord. (**J**) Axial view of the postoperative T_2 image, no compression to the spinal cord was observed (white arrow indicates the implant). (**K, L**) Hardware enhanced reconstruction of postoperative CT.

Co., Ltd, Beijing, China) and tested as the fixation group. All of the specimens were kept moist with 0.9% saline during the testing. The average ROM of at least three circles recorded by Opotrack Certus was used for data analysis.

Statistical analysis

Data is presented as mean ±SD. The statistical analysis was performed using SPSS 19.0. One-way ANOVA with Bonferroni's post-hoc test was used to analyze ROM. A *p*-value of less 0.05 was considered statistically significant. The statistical tests were

intended to find possible differences among groups, not to establish an overall superiority of one technique compared with another. Therefore, *p* values were left unadjusted.

Results

Imagiological results

Postoperative x-ray images are shown in Figure 4A, 4B. The implants appear in proper position. No dislocation of the implants
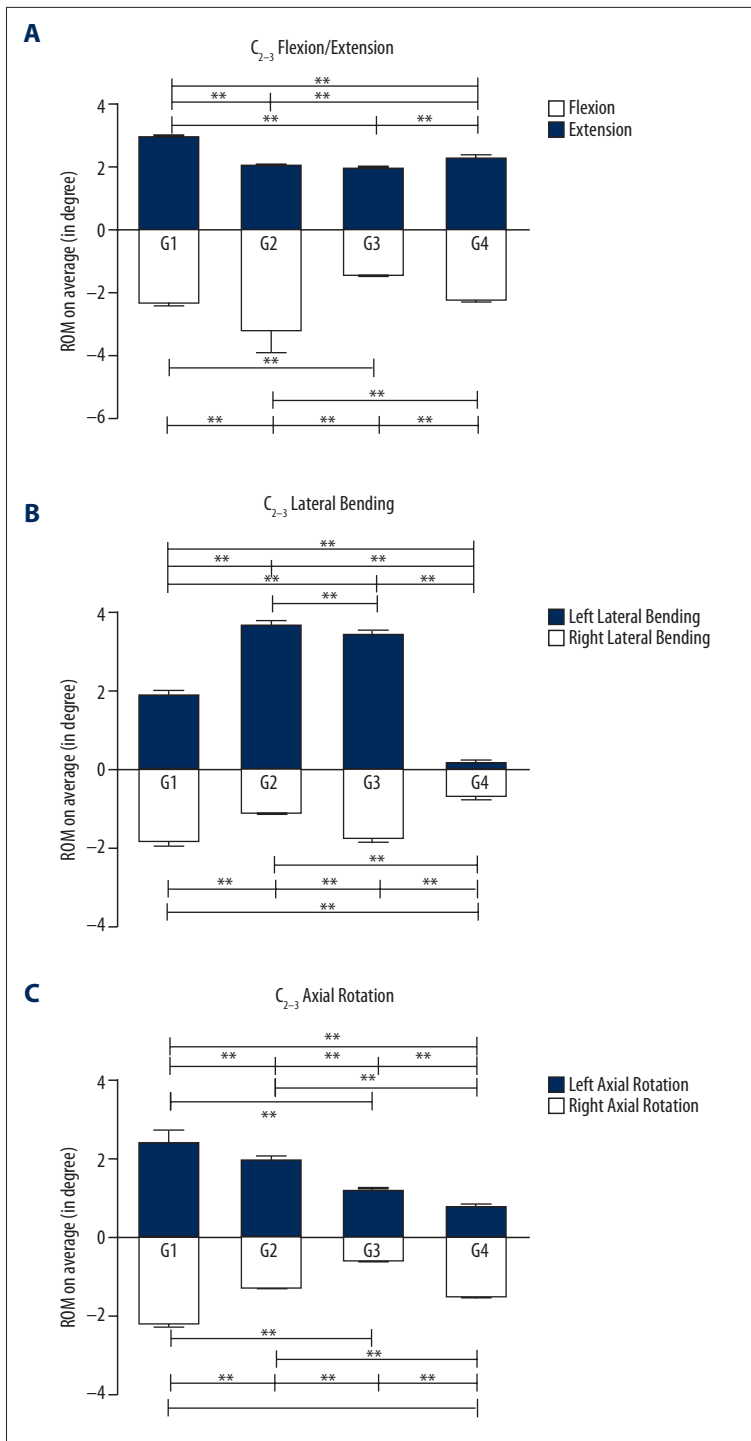
Figure 5. C_{2-3} ROM histogram. G1 – Intact group. G2 – Fixation group. G3 – *In vivo* group. G4 – *In vitro* group. (**A**) C_{2-3} ROM in flexion and extension. (**B**) C_{2-3} ROM in left-right lateral bending. (**C**) C_{2-3} ROM in left-right axial rotation. ROM in flexion was highest in fixation group while the lowest in the *in vivo* group. The ROM in extension was higher in intact group but lower in the *in vivo* group. The *in vitro* group had the lowest ROM in lateral bending. ROMs in axial rotation of the four groups were significantly different. Two asterisks indicate *p*<0.01.

or loosened/fractured screws were observed. The postoperative 3D-CT showed that the height of the vertebra was reconstructed by the implant (Figure 4C–4F). The upper and lower artificial discs were firmly attached to the lower endplates. All of the screws were in the vertebra and did not enter into the spinal canal (Figure 4G, 4H). The postoperative MRI showed that the diameter of the spinal canal at the operative level did not change, suggesting no compression to the spinal cord (Figure 4I, 4J). 3D-CT at six months after the operation revealed the implant was still in good position (Figure 4K, 4L).
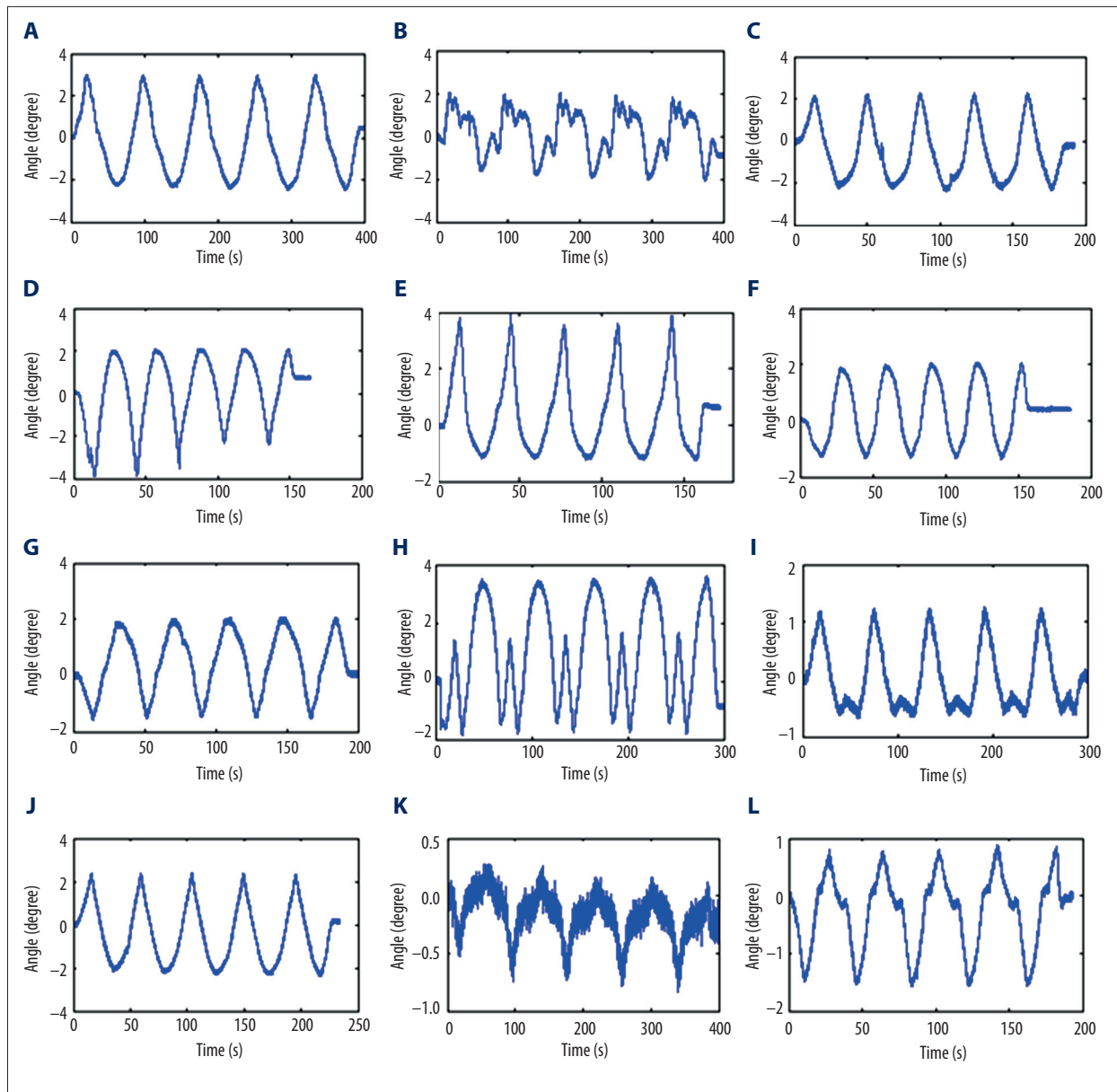
Supplementary Figure 1. C$_{2-3}$ ROM curve. ROM in flexion, right lateral bending and right axial rotation were recorded as negative, ROM in extension, left lateral bending and left axial rotation were recorded as positive. (**A**) Flexion and extension of the intact group. (**B**) Lateral bending of the intact group. (**C**) Axial rotation of the intact group. (**D**) Flexion and extension of the fixation group. (**E**) Lateral bending of the fixation group. (**F**) Axial rotation of the fixation group. (**G**) Flexion and extension of the *in vivo* group. (**H**) Lateral bending of the *in vivo* group. (**I**) Axial rotation of the *in vivo* group. (**J**) Flexion and extension of the *in vitro* group. (**K**) Lateral bending of the *in vitro* group. (**L**) Axial rotation of the *in vitro* group.

Biomechanics outcomes

C$_{2-3}$ ROM

The ROM of C$_{2-3}$ are shown in Figure 5 and Supplementary Figure 1. C$_{2-3}$ flexion in the fixation group was higher than the other three groups ($p<0.01$). C$_{2-3}$ flexion in the *in vivo* group was lower than the intact group and the *in vitro* group ($p<0.01$). No difference in C$_{2-3}$ flexion was observed between the intact group and the *in vitro* group ($p>0.05$). C$_{2-3}$ extension in the intact group was higher than the other three groups ($p<0.01$). C$_{2-3}$ extension in the *in vitro* group was also higher than in the fixation group and the *in vivo* group ($p<0.01$). No difference in C$_{2-3}$ extension was observed between the fixation group and
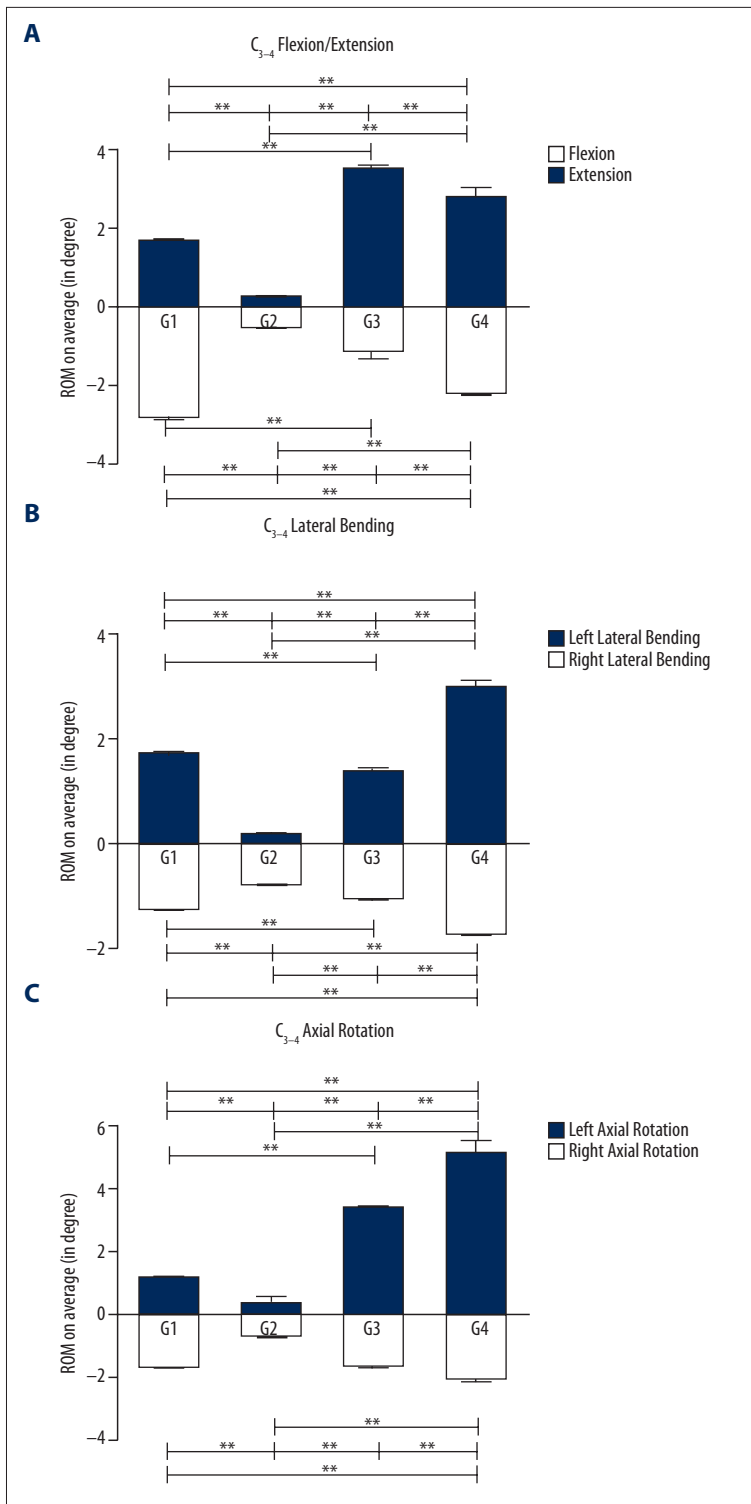
Figure 6. C_{3-4} ROM histogram. G1 – Intact group. G2 – Fixation group. G3 – *In vivo* group. G4 – *In vitro* group. (**A**) C_{3-4} ROM in flexion and extension. (**B**) C_{3-4} ROM in left-right lateral bending. (**C**) C_{3-4} ROM in left-right axial rotation. Fixation group had lowest ROM in all directions comparing with the other three groups. The *in vivo* group had the highest ROM in flexion while the intact group had the highest ROM in extension. The *in vitro* group had highest ROM in lateral bending and axial rotation. Two asterisks indicate $p<0.01$.

the *in vivo* group ($p>0.05$) (Figure 5A). Significant differences were observed in the pairwise comparison of C_{2-3} left lateral bending among the four groups. C_{2-3} ROM of left lateral bending was highest in the fixation group and lowest in the *in vitro* group (Figure 5B). C_{2-3} right lateral bending was lowest in the *in vitro* group. C_{2-3} axial rotation of the four groups were significantly different ($p<0.01$) (Figure. 5C).
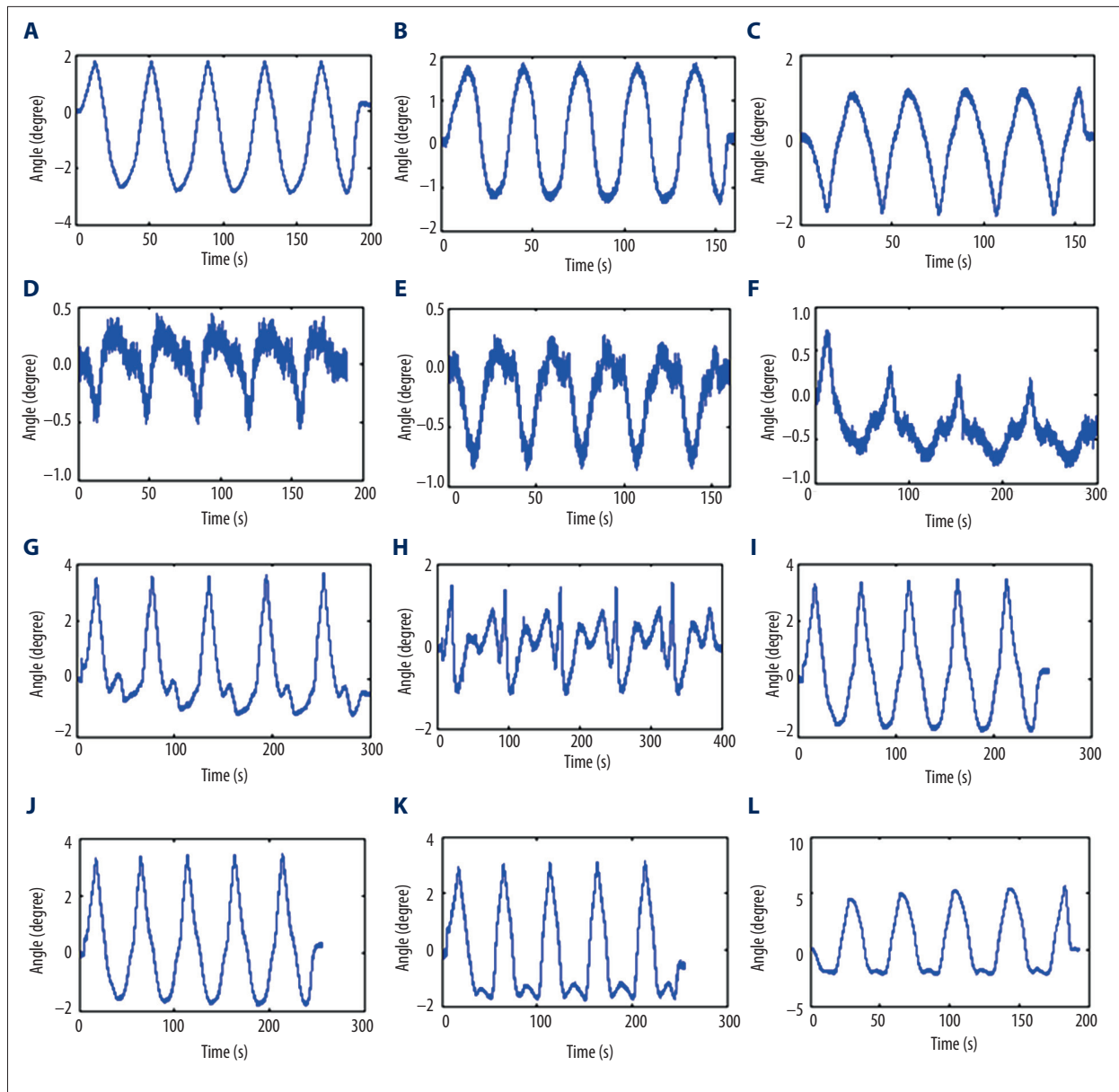
Supplementary Figure 2. C$_{3-4}$ ROM curve. ROM in flexion, right lateral bending and right axial rotation were recorded as negative, ROM in extension, left lateral bending and left axial rotation were recorded as positive. (**A**) Flexion and extension of the intact group. (**B**) Lateral bending of the intact group. (**C**) Axial rotation of the intact group. (**D**) Flexion and extension of the fixation group. (**E**) Lateral bending of the fixation group. (**F**) Axial rotation of the fixation group. (**G**) Flexion and extension of the *in vivo* group. (**H**) Lateral bending of the *in vivo* group. (**I**) Axial rotation of the *in vivo* group. (**J**) Flexion and extension of the *in vitro* group. (**K**) Lateral bending of the *in vitro* group. (**L**) Axial rotation of the *in vitro* group.

C$_{3-4}$ ROM

The ROM of C$_{3-4}$ are shown in Figure 6 and Supplementary Figure 2. C$_{3-4}$ ROM in all directions for the four groups was significantly different during pairwise comparison ($p<0.01$). The fixation group had the lowest C$_{3-4}$ ROM in all directions compared to the other three groups ($p<0.01$). The *in vivo* group had the highest C$_{3-4}$ flexion while the intact group had the highest C$_{3-4}$ extension (Figure 6A). The *in vitro* group had highest C$_{3-4}$ ROM for lateral bending and axial rotation (Figure 6B, 6C).
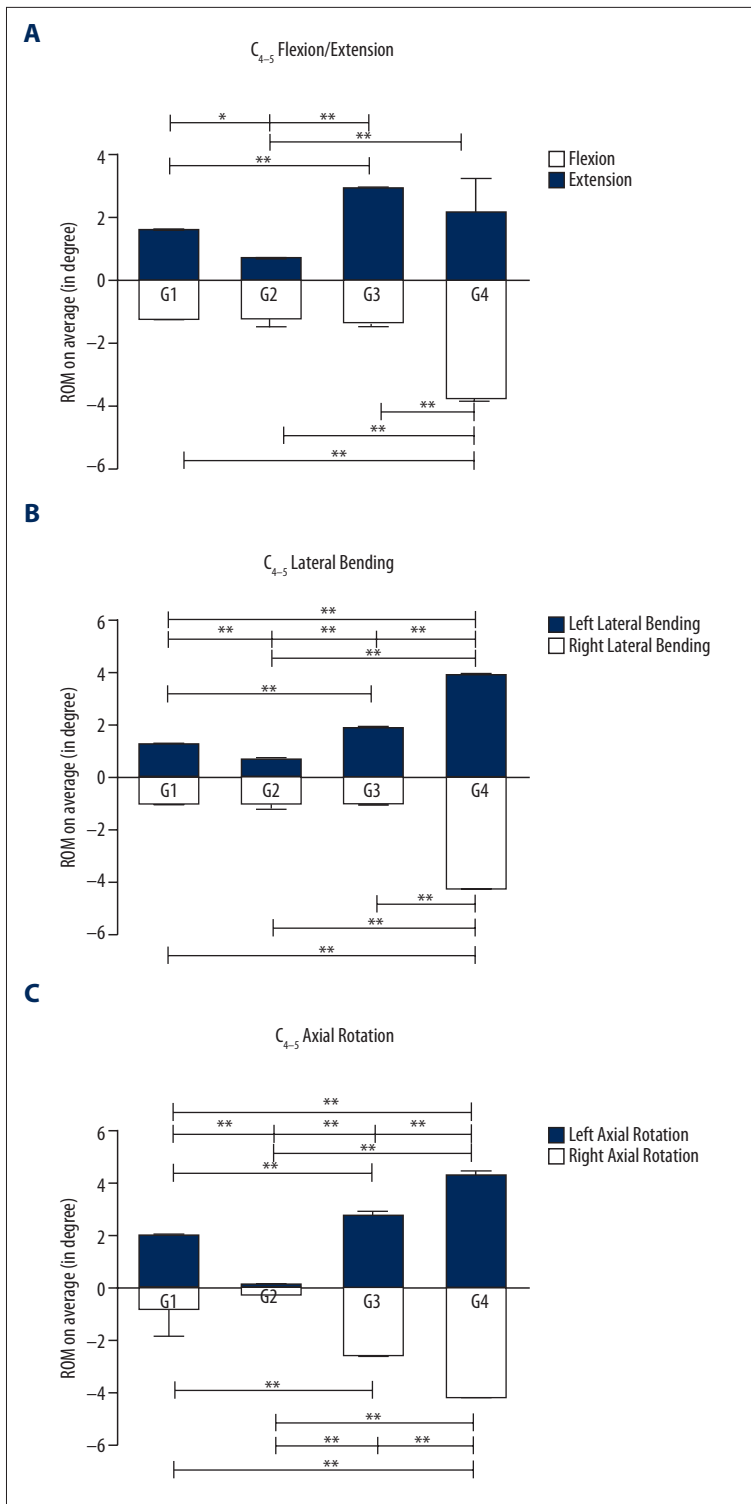
Figure 7. C$_{4-5}$ ROM histogram. G1 – Intact group. G2 – Fixation group. G3 – *In vivo* group. G4 – *In vitro* group. (**A**) C$_{4-5}$ ROM in flexion and extension. (**B**) C$_{4-5}$ ROM in left-right lateral bending. (**C**) C$_{4-5}$ ROM in left-right axial rotation. One asterisk indicates $p<0.05$. The *in vitro* group had the highest ROM in flexion and right lateral bending. ROM in extension was lowest in the fixation group while the highest in the *in vivo* group was higher than intact group. C$_{4-5}$ left lateral bending was significantly different in the pairwise comparison of the four groups. C$_{4-5}$ ROM in axial rotation was highest in the *in vitro* group and lowest in the fixation group. ROM in axial rotation was highest in the *in vitro* group and lowest in the fixation group. Two asterisks indicate $p<0.01$.

C$_{4-5}$ ROM

The ROM of C$_{4-5}$ are shown in Figure 7 and Supplementary Figure 3. C$_{4-5}$ ROM flexion and right lateral bending of the *in vitro* group was higher than the other three groups ($p<0.01$)

(Figure 7A, 7B). The C$_{4-5}$ ROM in extension of the fixation group was lower than in the other three groups. C$_{4-5}$ extension of the *in vivo* group was higher than the intact group. C$_{4-5}$ left lateral bending was significantly different in the pairwise comparison of the four groups (Figure 7B). C$_{4-5}$ ROM in axial rotation was
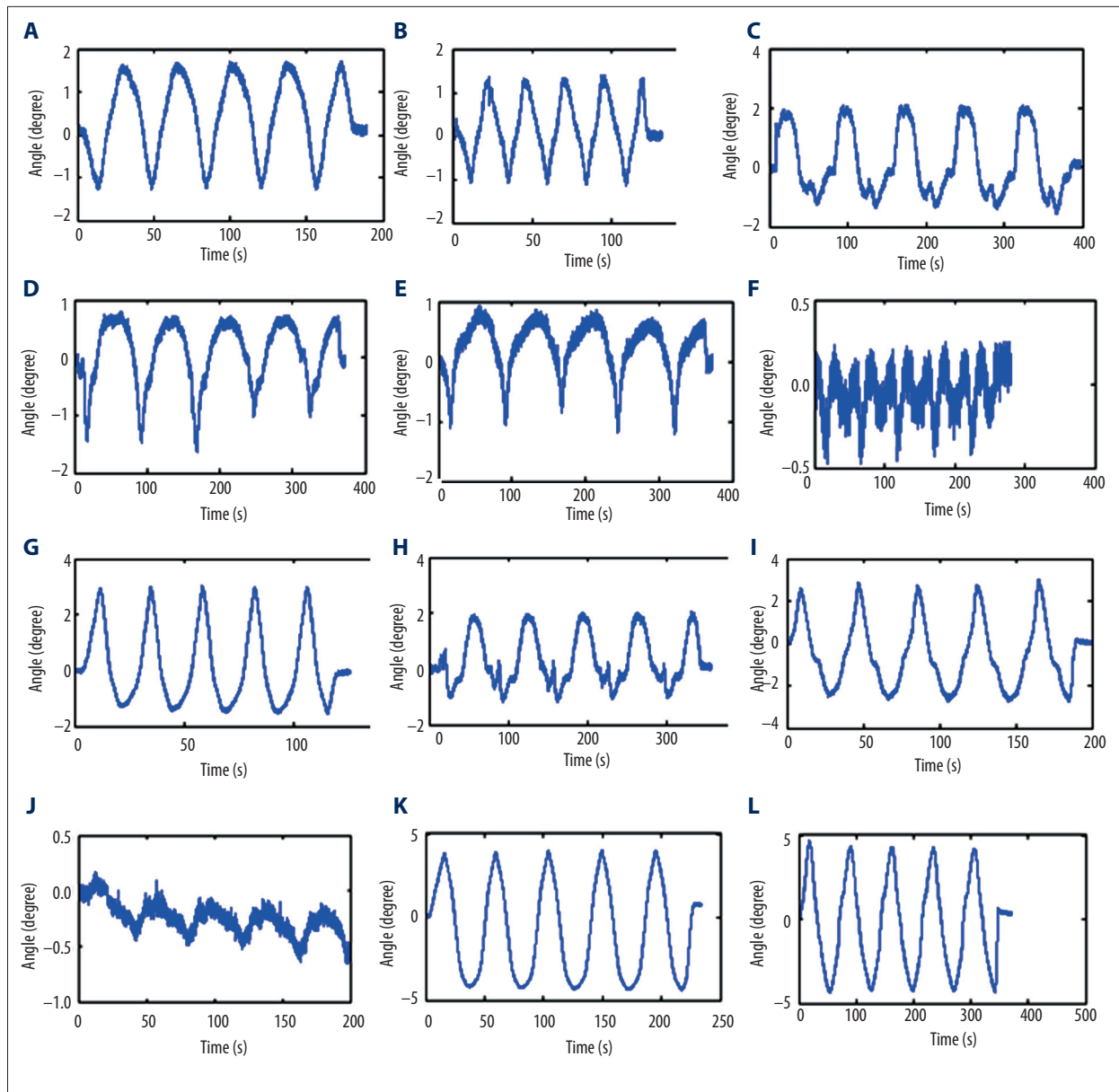
Supplementary Figure 3. C$_{4-5}$ ROM curve. ROM in flexion, right lateral bending and right axial rotation were recorded as negative, ROM in extension, left lateral bending and left axial rotation were recorded as positive. (**A**) Flexion and extension of the intact group. (**B**) Lateral bending of the intact group. (**C**) Axial rotation of the intact group. (**D**) Flexion and extension of the fixation group. (**E**) Lateral bending of the fixation group. (**F**) Axial rotation of the fixation group. (**G**) Flexion and extension of the *in vivo* group. (**H**) Lateral bending of the *in vivo* group. (**I**) Axial rotation of the *in vivo* group. (**J**) Flexion and extension of the *in vitro* group. (**K**) Lateral bending of the *in vitro* group. (**L**) Axial rotation of the *in vitro* group.

highest in the *in vitro* group and lowest in the fixation group (Figure 7C). Significant differences were observed in pairwise comparison of C$_{4-5}$ left axial rotation among the four groups ($p<0.01$). Similarly, significant differences were observed in pairwise comparison in C$_{4-5}$ right axial rotation among the four groups ($p<0.01$) except between the intact group and the fixation group (Figure 7C).

C$_{2-5}$ ROM

The ROM of C$_{4-5}$ is shown in Figure 8 and Supplementary Figure 4. C$_{2-5}$ ROM in flexion and extension were the lowest in the fixation group and the highest in the *in vitro* group. Significant differences were detected in C$_{2-5}$ ROM in flexion in the pairwise comparison among four groups ($p<0.01$) (Figure 8). Significantly
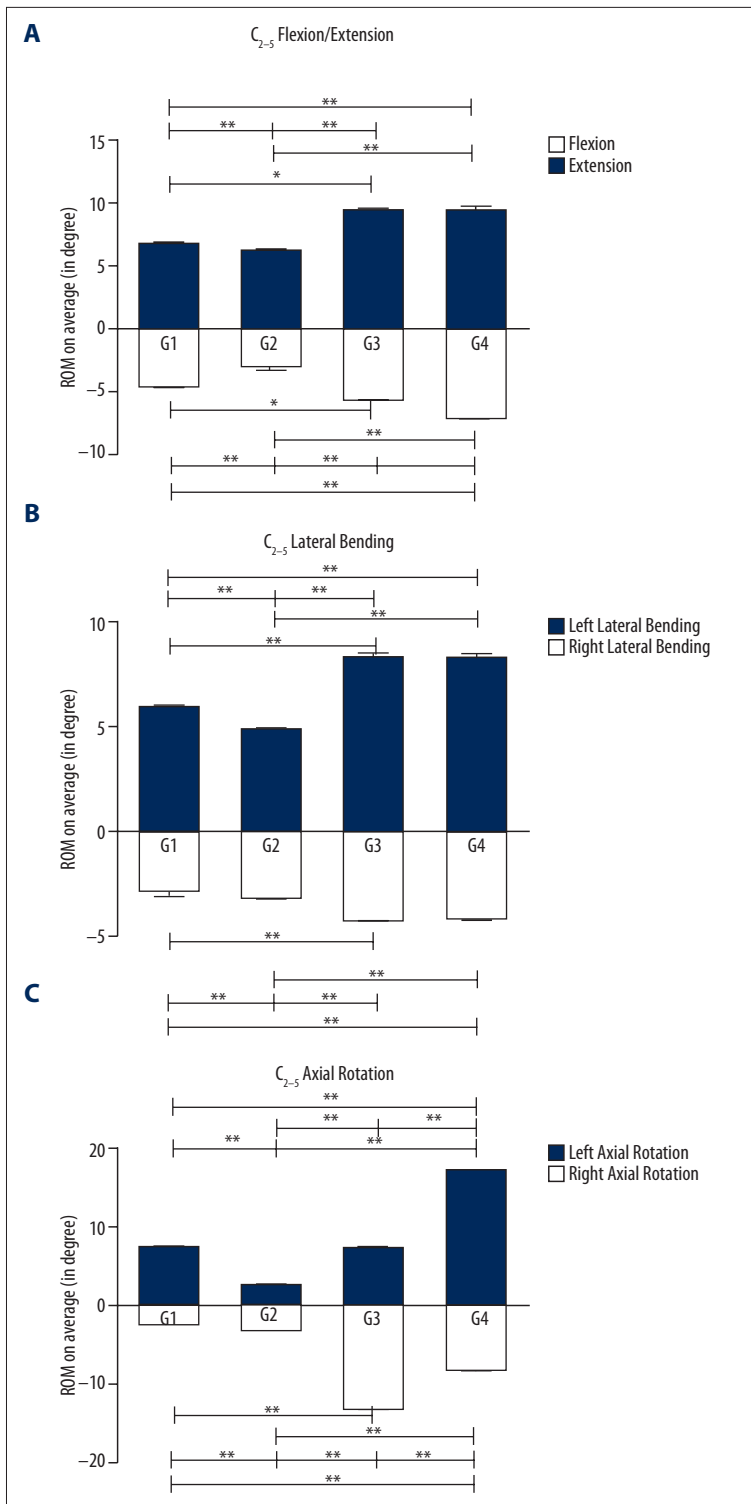
Figure 8. C_{2-5} ROM histogram. G1 – Intact group. G2 – Fixation group. G3 – *In vivo* group. G4 – *In vitro* group. (**A**) C_{2-5} ROM in flexion and extension. (**B**) C_{2-5} ROM in left-right lateral bending. (**C**) C_{2-5} ROM in left-right axial rotation. One asterisk indicates $p<0.05$. ROM in flexion and extension were the lowest in the fixation group and the highest in the *in vitro* group. ROM in lateral bending in the *in vivo* group or the *in vitro* group was significantly different from the intact or the fixation group. ROM in axial rotation was the lowest among the four groups. Significant increased ROM in left axial rotation was observed in the *in vitro* group compared with the other three groups. Significant differences were detected in ROM in right axial rotation in the pairwise comparison among four groups. Two asterisks indicate $p < 0.01$.

increased C_{2-5} ROM in extension was observed in the *in vivo* or *in vitro* group compared with the intact or the fixation group ($p<0.01$) (Figure 8A). No difference was detected in C_{2-5} ROM in extension between the *in vivo* and the *in vitro* group ($p>0.05$) (Figure 8A). C_{2-5} ROM in left and right lateral bending in the *in*

vivo group or the *in vitro* group was significantly different from the intact or the fixation group ($p<0.01$) (Figure 8B). No difference in C_{2-5} ROM in lateral bending was detected between the *in vivo* group and the *in vitro* group ($p>0.05$). C_{2-5} ROM in left and right axial rotation was the lowest among the four
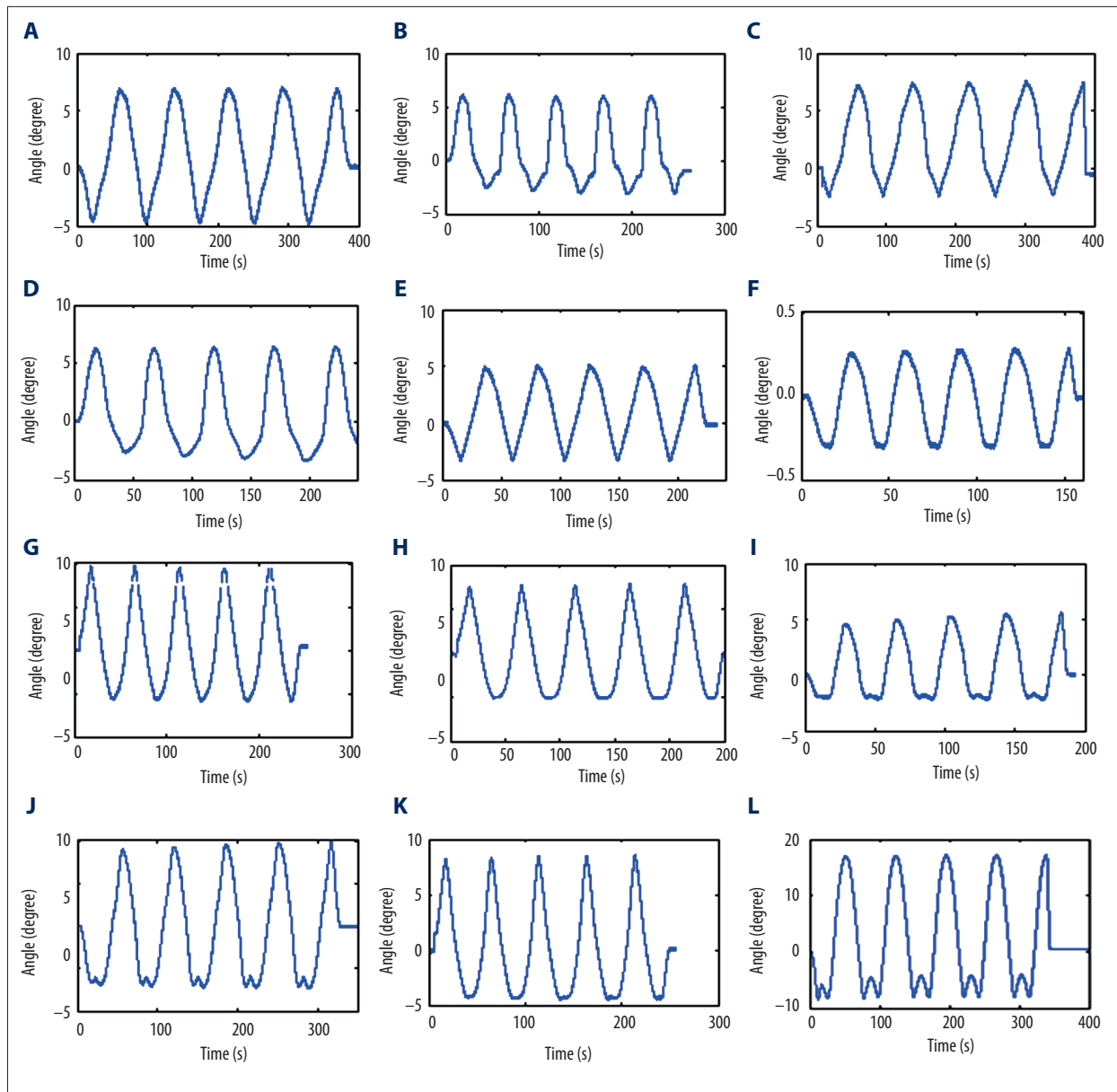
Supplementary Figure 4. C_{2-5} ROM curve. ROM in flexion, right lateral bending and right axial rotation were recorded as negative, ROM in extension, left lateral bending and left axial rotation were recorded as positive. (**A**) Flexion and extension of the intact group. (**B**) Lateral bending of the intact group. (**C**) Axial rotation of the intact group. (**D**) Flexion and extension of the fixation group. (**E**) Lateral bending of the fixation group. (**F**) Axial rotation of the fixation group. (**G**) Flexion and extension of the *in vivo* group. (**H**) Lateral bending of the *in vivo* group. (**I**) Axial rotation of the *in vivo* group. (**J**) Flexion and extension of the *in vitro* group. (**K**) Lateral bending of the *in vitro* group. (**L**) Axial rotation of the *in vitro* group.

groups (Figure 8C). Significant increased C_{2-5} ROM in left axial rotation was observed in the *in vitro* group compared with the other three groups ($p < 0.01$) (Figure 8C). Significant differences were detected in C_{2-5} ROM in right axial rotation in the pairwise comparison among four groups ($p < 0.01$) (Figure 8C).

Discussion

The present study established an anterior cervical corpectomy (ACC) non-fusion animal model in goats. Experimentally, the implantation of a novel implant preserved the ROM of the operative levels and reduced the ROM of the upper adjacent level of the specimen; these conditions may be related to the

lower risk of developing ASD. In summary, this study reports on a successful method of ACC non-fusion modelling, which provides a new way for future study of non-fusion treatment strategies of cervical spinal disease. The authors believe the model reported in this study is a reliably reproducible non-fusion model after cervical corpectomy. Our study results suggests this new approach may be an alternative to anterior fusion method.

ACCF is an effective strategy for cervical spinal disease [1,2]. This approach is frequently used in the treatment of multi-level cervical spondylotic myelopathy. ACCF usually includes a corpectomy and implants of an end-construct plate fixation spanning the strut graft. Notably, the biomechanical environment is greatly changed after rigid fusion of three or more vertebras, which generates a large moment arm at the ends of the construct [10]. The most visible alteration of the cervical spine is the motor function. A number of biomechanical studies have evaluated the cervical spine ROM after ACCF [11–14]. Galler et al. reported that corpectomy and grafting allowed the ROM of the fusion level to be dispersed fairly equivalently into the non-operative levels in flexion, lateral bending, and axial rotation [13].

Motion loss is a common feature caused by anterior fusion. Currently, non-fusion procedures, such as cervical disc arthroplasty, have been developed for preserving the ROM of the operative levels and have yielded favorable clinical outcomes [3]. However, insertion of an artificial cervical disc cannot reestablish the height of the vertebra, which makes this procedure impracticable for ROM preservation after a corpectomy. Currently, there is no anterior corpectomy non-fusion model due to the lacking of proper implants. The implant in our study has the function of reconstructing the vertebra height using the implantation of an artificial vertebra and preserving the ROM produced by the relative movement of the disc part and vertebra part. This non-fusion model provides an alternative procedure for the treatment of cervical spinal disease. The first goal of this unique procedure is to provide the cervical spine with a stable biomechanical environment by reconstruction the height of vertebra after corpectomy, which cannot be achieved by implanting artificial cervical disc or artificial nucleus [15]. The second goal is to restore the dynamic function of the intervertebral space by means of the motional structure of the novel implant. Theoretically, the non-fusion procedure could decrease the ROM of the adjacent levels due to the preservation of the ROM at the corpectomy level. Previous studies reported that the increased ROM of the adjacent level was related to a high risk of developing adjacent segment disease (ASD) [16–19]. The corpectomy non-fusion model has the potential to ameliorate ASD.

In this study, we reported the six-degrees-of-freedom ROM of the goat cervical spine under four experimental conditions. The biomechanical testing of *in vitro* models are very important; if the *in vitro* prosthesis has no ROM or shows catastrophic results such as dislocation, it cannot be used *in vivo*. Thus, an *in vivo* model must be established based on the results of an *in vitro* model. This study used both *in vitro* and *in vivo* models. We also wanted to know whether the two models had different ROM when, after several months, the soft tissue of the *in vivo* model may affect the ROM. According to Watson et al., the ROM in flexion of the three groups was not equal to the extension because goats have larger ROM in flexion than extension [20]; similar result was observed in our study. In general, the ROM of the left movement should be equal to the right movement. However, a symmetrical motion curve was not observed. Possible reasons for this discrepancy are as follows. First, the embedding of the specimens into the mold requires a stable fixation and a high accuracy of a neutral position of the specimens, which are difficult to achieve. Second, although the goats for specimen harvesting were the same age and similar body weight, the anatomical structure of the goat cervical spines were not completely the same. Third, the implantation of the implant affects the symmetry of the specimens if the position of the implant is not in the centerline of the cervical spine.

Despite the motion preservation, another important function for a successful non-fusion model is to provide stability for the cervical spine. The model will be considered unstable if the ROM of the non-fusion segments is too large, which is particularly dangerous for the cervical spinal cord – the ROM should be neither too large nor too small. In this study, the hemispheric articular fossae in the center of the two ends of artificial vertebra body were designed to prevent the dislocation of the disc and vertebra parts. This special design of the angle between the anterior plate and the endplate allowed the artificial disc part to firmly attach to the adjacent vertebra. Two lateral long grooves and two holes were designed for long-term bony fusion. Meanwhile, dentate grooves on the surface of the endplate might be more prone to bone ingrowth into the endplates, which reduces the risk of displacement. However, the specimens in the *in vivo* and the *in vitro* groups had significantly increased ROM compared with those in the intact group indicating that improvement of the model may be needed. Similarly, facet dislocation might happen if the axial ROM is too large [21].

This study had the following limitations. First, although the ROM of the operative levels could be preserved by implanting a novel implant, the different anatomical structures may require different sizes of implants. Second, the goat model established in this study might not have the same biomechanical properties of human models.

Conclusions

The presented implant model provides a better understanding of the potential motion loss after anterior fusion, and the potential to develop a new non-fusion device for the treatment of cervical spinal disease. Further research will be necessary to understand the biocompatibility and tribological properties of this implant model.

Statement

The authors declare that they have no competing interests. All the co-authors had participated sufficiently in the work to take public responsibility for appropriate portions of the content.

References:

1. Kimura H, Shikata J, Odate S, Soeda T: Anterior corpectomy and fusion to C_2 for cervical myelopathy: Clinical results and complications. Eur Spine J, 2014; 23: 1491–501

2. Yang HS, Chen DY, Lu XH et al: Choice of surgical approach for ossification of the posterior longitudinal ligament in combination with cervical disc hernia. Eur Spine J, 2010; 19: 494–501

3. Kan L, Kang J, Gao R et al: Clinical and radiological results of two hybrid reconstructive techniques in noncontiguous 3-level cervical spondylosis. J Neurosurg Spine, 2014; 21: 944–50

4. Liu J, Chen X, Liu Z et al: Anterior cervical discectomy and fusion versus corpectomy and fusion in treating two-level adjacent cervical spondylotic myelopathy: A minimum 5-year follow-up study. Arch Orthop Trauma Surg, 2015; 135: 149–53

5. Chung JY, Kim SK, Jung ST, Lee KB: Clinical adjacent-segment pathology after anterior cervical discectomy and fusion: Results after a minimum of 10-year follow-up. Spine J, 2014; 14: 2290–98

6. Kretzer RM, Hsu W, Hu N et al: Adjacent-level range of motion and intradiscal pressure after posterior cervical decompression and fixation: An *in vitro* human cadaveric model. Spine (Phila Pa 1976), 2012; 37: E778–85

7. Robertson JT, Papadopoulos SM, Traynelis VC: Assessment of adjacent-segment disease in patients treated with cervical fusion or arthroplasty: A prospective 2-year study. J Neurosurg Spine, 2005; 3: 417–23

8. Phillips FM, Lee JY, Geisler FH et al: A prospective, randomized, controlled clinical investigation comparing PCM cervical disc arthroplasty with anterior cervical discectomy and fusion. 2-year results from the US FDA IDE clinical trial. Spine (Phila Pa 1976), 2013; 38: E907–18

9. Lei T, Shen Y, Wang LF et al: Anterior longitudinal decompression in the management of severe ossification of the posterior longitudinal ligament in the cervical spine. Orthopedics, 2014; 37: e465–72

10. Singh K, Vaccaro AR, Kim J et al: Enhancement of stability following anterior cervical corpectomy: A biomechanical study. Spine (Phila Pa 1976), 2004; 29: 845–49

11. Karam YR, Dahdaleh NS, Magnetta MJ et al: Biomechanical comparison of anterior, posterior, and circumferential fixation after one-level anterior cervical corpectomy in the human cadaveric spine. Spine (Phila Pa 1976), 2011; 36: E455–60

12. Hussain M, Nassr A, Natarajan RN et al: Relationship between biomechanical changes at adjacent segments and number of fused bone grafts in multilevel cervical fusions: A finite element investigation. J Neurosurg Spine, 2014; 20: 22–29

13. Galler RM, Dogan S, Fifield MS et al: Biomechanical comparison of instrumented and uninstrumented multilevel cervical discectomy versus corpectomy. Spine (Phila Pa 1976), 2007; 32: 1220–26

14. Ulmar B, Disch A, Erhart S, Schmoelz W: Biomechanical analysis of anterior stabilization techniques for different partial and total vertebral corpectomy defect models. Biomed Tech (Berl), 2012; 57: 149–55

15. Burkus JK, Traynelis VC, Haid RW Jr., Mummaneni PV: Clinical and radiographic analysis of an artificial cervical disc: 7-year follow-up from the Prestige prospective randomized controlled clinical trial: Clinical article. J Neurosurg Spine, 2014; 21: 516–28

16. Anderst WJ, Donaldson WF III, Lee JY, Kang JD: Cervical motion segment contributions to head motion during flexion\extension, lateral bending, and axial rotation. Spine J, 2015; 15: 2538–43

17. Uddanapalli SS: New classification for clinically symptomatic adjacent segment pathology in cervical disc disease. Asian Spine J, 2015; 9: 942–51

18. Virk SS, Niedermeier S, Yu E, Khan SN: Adjacent segment disease. Orthopedics, 2014; 37: 547–55

19. Zhang JT, Cao JM, Meng FT, Shen Y: Cervical canal stenosis and adjacent segment degeneration after anterior cervical arthrodesis. Eur Spine J, 2015; 24: 1590–96

20. DeVries Watson NA, Gandhi AA et al: Sheep cervical spine biomechanics: A finite element study. Iowa Orthop J, 2014; 34: 137–43

21. Bodman A, Chin L: Bony fusion in a chronic cervical bilateral facet dislocation. Am J Case Rep, 2015; 16: 104–8